PEGylation of nanoparticles improves their cytoplasmic transport

Junghae Suh[1]
Kok-Leong Choy[1]
Samuel K Lai[2]
Jung Soo Suk[1]
Benjamin C Tang[2]
Sudhir Prabhu[2]
Justin Hanes[1,2,3]

[1]Department of Biomedical Engineering; [2]Department of Chemical and Biomolecular Engineering; [3]The Institute for NanoBioTechnology, The Johns Hopkins University, Baltimore, MD, USA

Abstract: The efficacy of nucleus-targeted drug- or gene-carrying nanoparticles may be limited by slow transport through the molecularly crowded cytoplasm following endosome escape. Cytoskeletal elements and cellular organelles may pose steric and/or adhesive obstacles to the efficient intracellular transport of nanoparticles. To potentially reduce adhesive interactions of colloids with intracellular components, the surface of model nanoparticles was coated with polyethylene glycol (PEG). Subsequently, multiple-particle tracking (MPT) was used to quantify the cytoplasmic transport rates of particles microinjected into the cytoplasm of live cells. PEGylation increased average nanoparticle diffusivities by 100% compared to unPEGylated particles (time scale of 10 s) in live cells. Faster particle transport correlated with a marked decrease in the number of particles that underwent hindered transport, from 79.2% (unmodified) to 48.8% (PEGylated). This result adds to an impressive list of positive benefits associated with PEGylation of drug and gene delivery vectors.

Keywords: PEG, polystyrene, particle tracking, cytoplasm, microinjection

Introduction

Targeted intracellular delivery of drugs and genes to the cell nucleus involves the transport of delivery vehicles through the crowded cytoplasm (Lechardeur et al 2005; Pack et al 2005). In addition to steric hindrances, adhesive interactions with intracellular components may act to significantly reduce the cytoplasmic transport rates of therapeutic colloids. Nonviral polyethylenimine (PEI)/DNA nanocomplexes are actively transported along microtubules to the perinuclear region of cells within 30 minutes post-transfection (Suh et al 2003). However, vectors that successfully escape endosomes in the perinuclear region of cells may still have to traverse distances of up to several micrometers through the molecularly crowded cytoplasm prior to reaching nuclear pore complexes, the entryway into the nucleus. Therefore, inefficient transport of particles outside of endosomes may critically limit effective drug and gene therapies.

Surface-modification of delivery vehicles with polyethylene glycol (PEG), or PEGylation, has shown promise as a method to improve the stability and in vivo performance of various non-viral drug and gene vectors (Sanders et al 2002; Ogris et al 2003; Lenter et al 2004; Mishra et al 2004; Pun et al 2004; Sun et al 2005; Zahr et al 2005). In addition, PEGylation has recently been shown to dramatically improve particle transport through biological obstacles, such as mucus from healthy volunteers (Lai et al 2007) or patients with cystic fibrosis (Hanes et al 2004). We hypothesized that PEGylation of therapeutic colloids may also improve their cytoplasmic transport (once the particles have escaped endosomal vesicles) by minimizing attractive forces to cytoskeletal elements, such as microtubules or actin filaments, or to other intracellular organelles. Here, multiple particle tracking (MPT) (Suh et al 2003, 2004, 2005) is used to compare the real time transport rates of individual PEGylated and unPEGylated polymeric nanoparticles in live cells.

Correspondence: Justin Hanes
Department of Chemical and Biomolecular Engineering, The Johns Hopkins University, 3400 N. Charles St., Baltimore, MD 21218, USA
Tel +1 410 516 3484
Fax +1 410 516 5510
Email hanes@jhu.edu

Materials and methods

Cell culture

HeLa cells (American Type Culture Collection, Manassas, VA) were cultured at 37 °C in 5% CO_2 in minimum essential medium (MEM, Invitrogen Corp., Carlsbad, CA) supplemented with 10% fetal bovine serum (FBS, Invitrogen Corp., Carlsbad, CA) and 1% penicillin/streptomycin (Invitrogen Corp., Carlsbad, CA). Cells were grown on 35-mm glass-bottom dishes (MatTek Corp., Ashland, MA).

Covalent PEGylation of nanoparticles

Di-amine polyethylene glycol (PEG) of molecular weight 3,400 daltons (Nektar Therapeutics, San Carlos, CA) was dissolved in 50 mM 2-(N-morpholino)ethanesulfonic acid (MES, Sigma, St Louis, MO) buffer at pH 6.0. The use of di-amine PEG may result in a free amine group at the end of the surface-bound PEG chains. Yellow-green fluorescent polystyrene nanospheres (Molecular Probes, Eugene, OR) were added to the solution to give final concentrations of 10 mg PEG/ml and 1% solids/ml. The nanospheres had diameters of 100 nm and were carboxyl-modified. Following a 15 min incubation at room temperature, 1-ethyl-3-(3-dimethylaminopropyl)-carbodiimide (EDAC, Sigma, St Louis, MO) was added to the mixture to a concentration of 4 mg/ml. The pH of the solution was adjusted to 6.5 with dilute NaOH and incubated on an orbital shaker for 2 h at room temperature. To quench the reaction, glycine (JT Baker, Phillipsburg, NJ) was added to give a final concentration of 100 mM. The solution was incubated for 30 min at room temperature and subsequently dialyzed extensively against Dulbecco's phosphate-buffered saline (PBS) in a 300,000 kDa MWCO Float-a-lyzer (Spectrum Laboratories, Rancho Dominguez, CA). Unmodified microspheres were dialyzed similarly to remove all traces of sodium azide originally added by the manufacturer.

Microinjection of particles

Prior to microinjection, solutions of PEGylated (PS-PEG) and unmodified nanospheres (PS) were diluted to approximately 1.8×10^7 particles/ml in distilled water, filtered through a 0.22 µm syringe filter (Millipore, Billerica, MA) and stored at 4 ºC. Nanospheres were injected using an Eppendorf Femto-Jet™ (Brinkmann Instruments, Westbury, NY) at a pressure of 180 hPa for 1.5s. Microinjection needles, Femtotips I (Brinkmann Instruments, Westbury, NY), were backloaded with 10 µl of particle solution using microloader pipetters (Brinkmann Instruments, Westbury, NY). Cells were microinjected at 37 °C in tissue culture medium supplemented with 150 mM

HEPES (Sigma, St Louis, MO). To facilitate the location of microinjected cells for microscopy, cells were microinjected only in the vicinity of a cross-mark inscribed onto the dish with a diamond-tipped glass scribe. After microinjection, cells were immediately washed twice with PBS, supplied with fresh tissue culture medium, and incubated for 2 h before observation under fluorescence microscopy.

Endocytosis of particles

HeLa cells were incubated in the presence of approximately 1.8×10^{10} PS particles in 1 mL of cell culture media for 3 h at 37 °C. Prior to observation under fluorescence microscopy, cells were washed twice with PBS and new media added.

Fluorescence microscopy and multiple particle tracking

Cells were maintained at 37 °C with an air stream stage incubator (Nevtek, Burnsville, VA) and observed with an inverted epifluorescence microscope, Axiovert (Carl Zeiss Inc., Thornwood, NY), equipped with a 100X/1.4 NA oil-immersion lens. Movies of particle transport in live HeLa cells were obtained at 15 frames per second with a Princeton Pentamax camera (Roper Scientific, Trenton, NJ). The movies were analyzed with the Tracking Objects application in MetaMorph software (Universal Imaging Corp., Downingtown, PA) to obtain particle positions over time. This data was then used to calculate mean-square displacements (MSD) and effective diffusivities (D_{eff}) of individual particles as shown previously (Suh et al 2003; Suh et al 2004). Briefly, MSD and D_{eff} of individual particles in two dimensions are

$$MSD = <\Delta x^2 + \Delta y^2>. \qquad (1)$$

$$D_{eff} = MSD/(4\tau) \qquad (2)$$

where τ is time scale. Bulk transport properties were then obtained by ensemble-averaging individual transport rates. More detailed information on particle tracking can be found elsewhere (Suh et al 2005).

Results and discussion

Effect of PEGylation on cytoplasmic transport rates

In this study, we quantitatively investigated whether the cytoplasmic transport of nanoparticles can be improved by surface modification with PEG. The covalent conjugation of PEG onto the surface of model drug delivery particles, 100 nm polystyrene (PS) nanoparticles, doubles their average

transport rate in cells (at a time scale of 10s), as measured by ensemble-averaged mean-square displacement (Figure 1A) and ensemble-averaged diffusivity (Figure 1B). Time scale is the amount of time a particle is allowed to move before calculating its displacement from an initial position (Suh et al 2005), therefore, MSD increases with time (Figure 1A). Our group has shown PEGylation also improves particle transport rates by more than two orders of magnitude through cystic fibrosis mucus by reducing particle adhesion (Hanes et al 2004).

Average particle diffusivity values for both PS and PS-PEG decrease over time scale (Figure 1B), suggesting both types of nanoparticles experience sub-diffusive (or hindered) transport (Saxton 1994, 1996) in the cytoplasm of live cells. This is not surprising, since the cell cytoplasm is known to be a highly viscoelastic medium crowded with cytoskeletal elements, including microtubules and actin filaments (Tseng et al 2002). Actin networks can form tight meshes in certain areas of the cell, with a mean pore diameter of 50 nm (Luby-Phelps 1993, 2000).

To further characterize the differences in the intracellular transport of PS versus PS-PEG, the motions of individual nanoparticles were classified into three transport modes (Suh et al 2005): diffusive, active, and hindered (encompassing immobile and sub-diffusive particles).

Classification of transport modes

Kusumi and coworkers (Kusumi et al 1993) defined a stationary, or immobile, mode of transport that reflects the tight adhesion of the transporting species to rigid cellular components. The diffusivity of stationary proteins was obtained by assuming that the short-range motion of actively transporting species (in this case transmembrane proteins) is likely due to the small structural fluctuations of the cyto-skeleton to which the proteins are attached. (To be actively transported, the proteins need to be closely associated with cytoskeletal filaments, such as actin, that underlie the plasma membrane.) Unfortunately, a similar methodology could not be applied to the particles in this study since microtubules in the cytoplasm of cells can experience substantial thermal fluctuation (data not shown). Particles tightly adhered to microtubules, therefore, may display diffusivity values on the order of particles moving by diffusive or sub-diffusive modes. Multi-color confocal particle tracking studies are underway to directly visualize the interaction of particles with fluorescently labeled microtubules in live cells. These studies should help directly determine the extent to which particles adhere to cytoskeletal structures as well as estimate their transport rates. Until then, we have assigned particles as immobile if their diffusivities are not above background noise in the particle tracking system.

To determine the mode of transport (ie, diffusive, sub-diffusive, or active) of the mobile nanoparticles, a parameter called Relative Change (RC) is calculated for each particle. RC is defined as

$$RC = D_{eff, probed\ \tau}/D_{eff, reference\ \tau} \qquad (3)$$

where the reference time scale (τ) is smaller than the probed τ. Therefore, RC is a measure of the relative change in diffusivity (D_{eff}) of a single particle over time scale. In theory, particles moving by simple diffusion are expected to have constant diffusivities over time scale (or a RC value of 1). D_{eff} values increasing with time scale (RC values greater than 1) indicate actively transported particles, and D_{eff} values decreasing with time scale (or RC values less than 1) suggest sub-diffusive particles (Dawson et al 2003; Suh et al 2003, 2004, 2005).

Due to the random nature of diffusion, however, the RC values of a population of purely diffusive particles will have
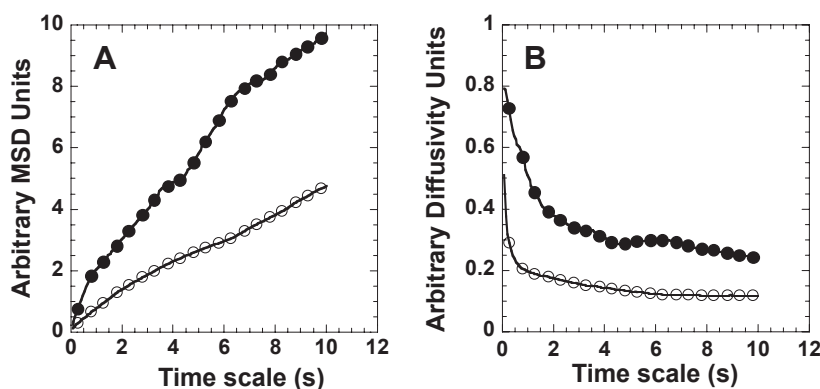

Figure 1 Average cytoplasmic transport rates of PS or PS-PEG nanoparticles microinjected into live HeLa cells. (**A**) Ensemble MSD or (**B**) ensemble diffusivity of PS (open circles, n = 101) or PS-PEG (closed circles, n = 86) nanoparticles.

a certain spread around the value 1. Therefore, a Monte Carlo simulation of 10,000 random walks was used to predict this distribution of RC values. Similar to other work in the literature, the Monte Carlo simulated random walks are based on a continuum model with a fixed step size and unrestricted angle of jump (Saxton 1994). The angle θ, between 0 and 2π, is generated with uniform probability and the tracer particle is moved at each fixed time interval Δτ by

$$\Delta x = L \cos(\theta); \qquad x_{\tau + \Delta \tau} = x_\tau + \Delta x \qquad (4)$$

$$\Delta y = L \sin(\theta); \qquad y_{\tau + \Delta \tau} = y_\tau + \Delta y \qquad (5)$$

where x and y are coordinates in 2-dimensional space and L is the step size. To match experimental conditions of 20 s-movies at 15 frames/s, each particle is simulated for 300 frames and the individual MSD, D_{eff}, and RC v. time scale (τ) are calculated. Because RC is a dimensionless quantity, the Monte Carlo findings can be related to experimental results without any conversion factor. Hence, the step size L was simply set to 1.

From this theoretical RC distribution of purely diffusive particles, upper and lower RC bounds are obtained by placing 95% of the values between the upper and lower bounds. Figure 2 shows the upper and lower RC bounds as dotted lines for short (Figure 2A) and long (Figure 2B) time scales. Under this criterion, 2.5% of the values are above the upper RC bound and 2.5% of the values are below the lower RC bound.

Next, by calculating the RC values of each microinjected particle for the two time regimes (ie, short and long time scales), one can obtain the transport mode that describes the particle transport properties over the different length scales. For example, if the RC^{short} for a microinjected particle falls below the lower RC bound in Figure 2A, the short-range motion of the particle is classified as sub-diffusive. Then,

if the RC^{long} for the same particle falls within the upper and lower RC bounds, the long-range motion of the particle is classified as diffusive. The overall transport mode of the particle is then categorized as sub-diffusive over the probed time (Table 1). In our application of tracking the motion of nanoparticles in cells, we found it useful to categorize the overall particle transport mode (based on values of RC^{short} and RC^{long}) according to Table 1. The overall transport mode categorization of a particle is also verified by visual inspection of its trajectory (Suh et al 2004).

Effect of PEGylation on particle transport modes

Based on the methodology from the previous section, the transport of microinjected nanoparticles was first categorized into immobile and mobile populations. Particles were classified as immobile if their diffusivities were indistinguishable from the noise in our experimental setup. The short-range and long-range transport of mobile particles was then further classified into three modes: diffusive, sub-diffusive, and active. Diffusive particles are undergoing unrestricted Brownian motion, sub-diffusive particles display hindered motion (possibly due to cytoplasmic obstacles, such as cytoskeletal structures), and actively transported particles likely experience motor protein-mediated transport along the cytoskeleton. Lastly, the immobile and sub-diffusive groups were combined into one hindered transport group.

The majority of both PS and PS-PEG nanoparticles experience hindered transport at short time scales (Figures 3A and 3C), suggesting the short-range motion of most particles is obstructed by the molecularly crowded microenvironment in the cell cytoplasm. A greater fraction of PEGylated nanoparticles, however, falls between the upper and lower bounds (Figure 3C), indicating a greater population of PEGylated particles exhibit purely diffusive behavior. At longer time scales, the particle transport mode
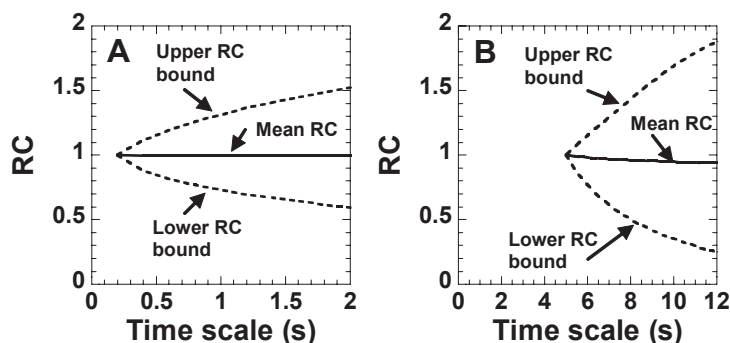

Figure 2 Upper and lower bounds for classifying 95% of 10,000 simulated random walks as purely diffusive. (**A**) Bounds for classifying the motion at short time scales as purely diffusive. RC is defined as $D_{\tau=1s} / D_{\tau=0.2s}$. (**B**) Bounds for classifying the motion at long time scales as purely diffusive. RC is defined as $D_{\tau=10s} / D_{\tau=5s}$.

Table 1 Classification of the overall particle transport mode based on the transport modes determined by RC^{short} and RC^{long} values. D = diffusive, S = sub-diffusive, A = active. Immobile and sub-diffusive particles are further grouped together as hindered particles.

		—— RC^{long} ——		
		D	**S**	**A**
	D	D	S	A
RC^{short}	**S**	S	S	A
	A	A	A	A

for both types of particles is predominantly diffusive (Figures 3B and 3D). Such transition from sub-diffusive to diffusive transport modes over time scale is possibly a reflection of the relaxation of the network structure (Mason et al 1997) defining the cytoplasmic microenvironment, and has been predicted for particles undergoing sub-diffusion due to the presence of obstacles (Saxton 1994). Alternatively, particles may be associating and dissociating from nonspecific binding sites in the cytoplasm.

The overall mode of transport of PS and PS-PEG particles was then determined based on the transport mode assignments at the short and long time scales (Table 1). Almost 80% of microinjected PS particles experience hindered transport in the cytoplasm of live cells (Figure 4), underscoring the potential difficulty in particle transport upon endosome escape. In contrast, only about 50% of PEGylated particles are classified as hindered. PEGylation of the nanoparticles increases the percentage of diffusive particles ~2-fold, from around 18% to 38%. It is possible the presence of PEG may reduce the adhesion of nanoparticles to cytoplasmic components, thereby affecting particle transport. Improved cytoplasmic transport of PEGylated particles may be due to reduced electrostatic interactions since PEGylation increases the particle zeta potential (in 10 mM NaCl) from −41 mV (unmodified PS) to −4 mV. PS nanoparticles are relatively hydrophobic in character; therefore, it is also possible that the increased hydrophilicity provided by the PEG coating is responsible for decreased van der Waals interactions with cytoplasmic components (Hanes et al 2003). The PEG coating may also act as a steric barrier to particle adsorption to intracellular components.

Unexpectedly, about 13% of PS-PEG particles are classified as actively transported compared to 3% for unmodified PS. Based on the statistical criteria set forth in the previous section, only about 2.5% of purely diffusive particles should be classified as active in order to be within expected error. It is possible that the 13% of PS-PEG particles categorized as actively transported were endocytosed during the microinjection, resulting in particles within endosomes. Previous work has shown polymeric gene vectors within endosomes experience active transport (Suh et al 2003). Several factors,
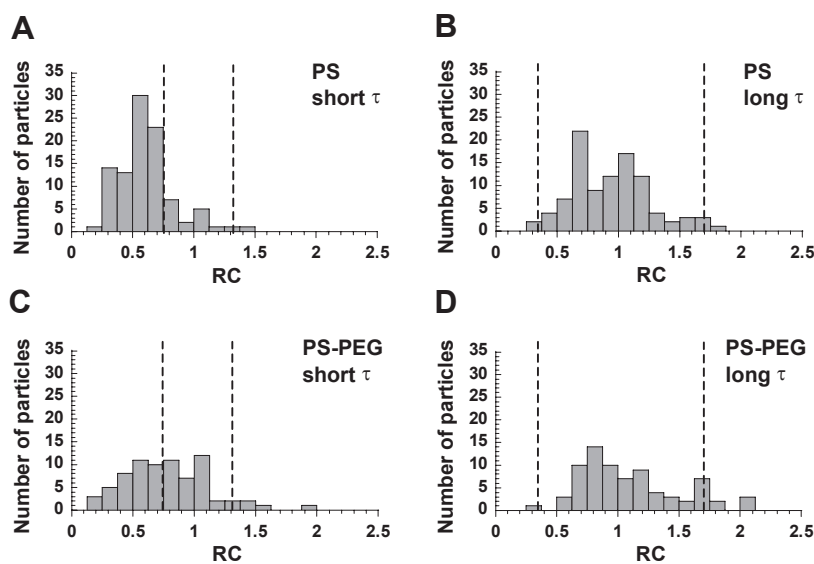

Figure 3 Relative change (RC) of particle diffusivities for mobile PS and PS-PEG particles. Values of RC at the (**A**) short time scale range (0.2–1 s) and (**B**) long time scale range (5–10 s) for PS particles microinjected into live HeLa cells. Values of RC at the (**C**) short time scale range (0.2–1 s) and (**D**) long time scale range (5–10 s) for PS-PEG particles microinjected into live HeLa cells. Upper and lower RC bounds for purely diffusive transport are indicated by vertical dotted lines. Particles with RC values that fall between these lines are classified as diffusive. Particles with RC values below the lower RC bound are classified as sub-diffusive, and those with RC values above the upper RC bound are classified as actively transported.
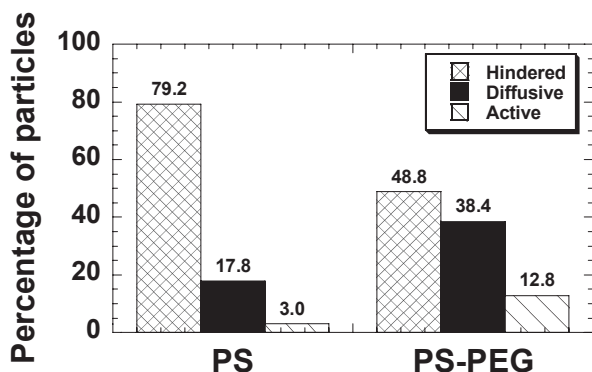
Figure 4 Overall transport modes of PS (n = 101) or PS-PEG (n = 86) nanoparticles microinjected into the cytoplasm of HeLa cells. The hindered group is composed of immobile and sub-diffusive particles.

however, make the endocytosis of PS-PEG during microinjection highly unlikely. First, carboxylated PS particles (as used in this study) are not internalized readily by cells and require greater than one-hour incubation in the presence of a high particle concentration to observe particle endocytosis (data not shown). The duration of microinjection in our studies lasts less than 30 minutes and the cells are washed twice and replenished with new media directly after microinjection. In addition, attachment of PEG to the surfaces of particles has been observed to decrease particle endocytosis (Ogris et al 2001).

When PS particles do enter cells via endocytosis (Figure 5), around 17% of particles are actively transported (Figure 5B), a value similar to that observed for endocytosed PEI/DNA nanoparticles (Suh et al 2003). Endocytosed PS particles display 4- and 9-fold greater average diffusivities (at time scale of 10 s) than PS-PEG and unmodified PS particles microinjected into the cytoplasm, respectively. Thus, even

with a similar percentage of particles classified as active (13% for microinjected PS-PEG versus 17% for endocytosed PS), the intracellular transport rates obtained for the two cases vary substantially. It is possible, although unlikely, that PS-PEG particles are able to attract cellular components necessary for active transport. Alternatively, actively transporting PS-PEG (although classified as "active") may be better classified as undergoing motor protein-independent directed transport. Directed particles may display an overall bias in the direction of their trajectory; however, this may be due to the structure of the environment surrounding the particle, rather than the action of motor proteins. Such environments may exist in certain areas of the cell where microtubules are highly organized (eg, close to the microtubule organizing center). This latter hypothesis is further supported by the observation that the trajectory of "actively transporting" PS-PEG particles often move an order-of-magnitude less than actively transporting PS particles that have been endocytosed. Therefore, the length scale of the particle trajectory may also need to be taken into account when classifying actively transporting particles.

In conclusion, PEGylation of polymeric nanoparticles improves their cytoplasmic transport rates (outside of endosomal vesicles), possibly by reducing non-specific adhesion to cytoskeletal elements. This property may be important in allowing drug/gene vectors, which have escaped endosomes, to efficiently reach the nucleus.
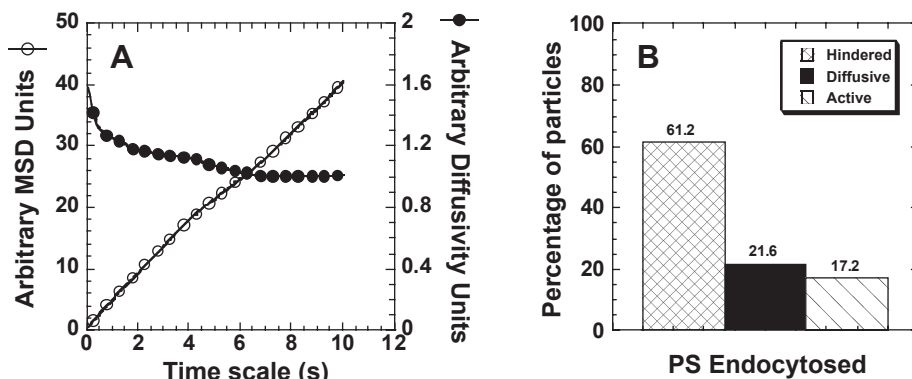
Acknowledgments

Figure 5 Transport characteristics of endocytosed PS particles. (**A**) Ensemble MSD (open circles) or ensemble diffusivity (closed circles) of endocytosed PS nanoparticles (n = 116) in live HeLa cells. (**B**) Overall transport modes of endocytosed PS particles.

References

Dawson M, Wirtz D, Hanes J. 2003. Enhanced viscoelasticity of human cystic fibrotic sputum correlates with increasing microheterogeneity in particle transport. *J Biol Chem,* 278:50393–401.

Hanes J, Dawson M, Har-el Y, et al. 2003. In Hickey AJ, ed. Pharmaceutical inhalation aerosol technology. New York: Marcel Dekker Inc. p 489–539.

Hanes J, Dawson M, Wirtz D, et al. Drugs and gene carrier particles that rapidly move through mucous barriers (US PCT pending; priority date: 28 January 2004).

Kusumi A, Sako Y, Yamamoto M. 1993. Confined lateral diffusion of membrane receptors as studied by single particle tracking (nanovid microscopy). Effects of calcium-induced differentiation in cultured epithelial cells. *Biophys J,* 65:2021–40.

Lai SK, O'Hanlon ED, Harrold S, et al. 2007. Rapid transport of large polymeric nanoparticles in fresh undiluted human mucus. *Proc Natl Acad Sci U S A,* 104:1482–7.

Lechardeur D, Verkman AS, Lukacs GL. 2005. Intracellular routing of plasmid DNA during non-viral gene transfer. *Advanced Drug Delivery Reviews,* 57:755–67.

Lenter MC, Garidel P, Pelisek J, et al. 2004. Stabilized nonviral formulations for the delivery of MCP-1 gene into cells of the vasculoendothelial system. *Pharmaceutical Research,* 21:683–91.

Luby-Phelps K. 1993. Effect of cytoarchitecture on the transport and localization of protein synthetic machinery. *J Cell Biochem,* 52:140–7.

Luby-Phelps K. 2000. Cytoarchitecture and physical properties of cytoplasm: Volume, viscosity. diffusion, intracellular surface area. *Internaltional Review of Cytology – A Survey of Cell Biology,* 192:189–221.

Mason TG, Ganesan K, vanZanten JH, et al. 1997. Particle tracking microrheology of complex fluids. *Physical Review Letters,* 79:3282–5.

Mishra S, Webster P, Davis ME. 2004. PEGylation significantly affects cellular uptake and intracellular trafficking of non-viral gene delivery particles. *European Journal of Cell Biology,* 83:97–111.

Ogris M, Steinlein P, Carotta S, et al. 2001. DNA/polyethylenimine transfection particles: Influence of ligands, polymer size, and PEGylation on international and gene expression. *Aaps Pharmsci,* 3, art. no.-21.

Ogris M, Walker G, Blessing T, et al. 2003. Tumor-targeted gene therapy: strategies for the preparation of ligand-polyethylene glycol-polyethylenimine/DNA complexes. *Journal of Controlled Release,* 91:173–81.

Pack DW, Hoffman AS, Pun S, et al. 2005. Design and development of polymers for gene delivery. *Nat Rev Drug Discov,* 4:581–93.

Pun SH, Tack F, Bellocq NC, et al. 2004. Targeted delivery of RNA-cleaving DNA enzyme (DNAzyme) to tumor tissue by transferrin-modified, cyclodextrin-based particles. *Cancer Biology and Therapy,* 3:641–50.

Sanders NN, De Smedt SC, Cheng SH, et al. 2002. Pegylated GL67 lipoplexes retain their gene transfection activity after exposure to components of CF mucus. *Gene Ther,* 9:363–71.

Saxton MJ. 1994. Anomalous diffusion due to obstacles: a Monte Carlo study. *Biophys J,* 66:394–401.

Saxton MJ. 1996. Anomalous diffusion due to binding: a Monte Carlo study. *Biophys J,* 70:1250–62.

Suh J, Dawson M, Hanes J. 2005. Real-time multiple particle tracking: applications to drug and gene delivery. *Adv Drug Deliv Rev,* 57:63–78.

Suh J, Wirtz D, Hanes J. 2003. Efficient active transport of gene nanocarriers to the cell nucleus. *Proc Natl Acad Sci U S A,* 100:3878–82.

Suh J, Wirtz D, Hanes J. 2004. Real-time intracellular transport of gene nanocarriers studied by multiple particle tracking. *Biotechnol Prog,* 20:598–602.

Sun XK, Rossin R, Turner JL, et al. 2005. An assessment of the effects of shell cross-linked nanoparticle size, core composition, and surface PEGylation on in vivo biodistribution. *Biomacromolecules,* 6:2541–54.

Tseng Y, Kole TP, Wirtz D. 2002. Micromechanical mapping of live cells by multiple-particle-tracking microrheology. *Biophys J,* 83:3162–76.

Zahr AS, de Villiers M, Pishko MV. 2005. Encapsulation of drug nanoparticles in self-assembled macromolecular nanoshells. *Langmuir,* 21:403–10.